

Lattice distortion of MnAs nanocrystals embedded in GaAs: Effect on the magnetic properties

M. Moreno^{a)}

Paul-Drude-Institut für Festkörperelektronik, Hausvogteiplatz 5-7, D-10117 Berlin, Germany and Instituto de Ciencia de Materiales de Madrid (CSIC), Cantoblanco, E-28049 Madrid, Spain

B. Jenichen, L. Däweritz, and K. H. Ploog

Paul-Drude-Institut für Festkörperelektronik, Hausvogteiplatz 5-7, D-10117 Berlin, Germany

(Received 20 December 2004; accepted 27 February 2005; published online 12 April 2005)

The x-ray coherent scattering in nanosized MnAs crystallites embedded in a GaAs matrix has been detected. The room-temperature interatomic distances along three orthogonal directions of the crystallites are determined. The MnAs nanocrystals are found to exhibit an anisotropically distorted hexagonal structure as compared to unstrained bulk MnAs. Despite the crystallite lattice distortion, the granular GaAs:MnAs material exhibits robust ferromagnetism, with enhanced transition temperature. The observed magnetic behavior is consistently explained by a localized double-exchange model of MnAs ferromagnetism, where magnetic order appears for large enough Mn–As–Mn distances, i.e., for weak enough *p-d* hybridization. © 2005 American Institute of Physics. [DOI: 10.1063/1.1899767]

Epitaxial MnAs films on GaAs and granular GaAs:MnAs, consisting of MnAs nanocrystals embedded in a GaAs matrix, are promising hybrid ferromagnet-semiconductor materials for information storage, magneto-optical, and spin-electronics applications.^{1–3} Bulk MnAs exhibits a complex magnetostructural phase diagram as a function of temperature and pressure.^{4–7} Most important, at approximately 313 K,⁷ bulk MnAs exhibits a first-order phase transition from a high-temperature paramagnetic orthorhombic MnP-type *B31* structure (β -phase) to a low-temperature ferromagnetic hexagonal NiAs-type *B8₁* structure (α -phase). Upon cooling across the first-order phase transition, an abrupt volume expansion of about 2% occurs, with the nearest-neighbor distance in the basal plane increasing abruptly and the nearest-neighbor distance along the *c* axis remaining unchanged. The mechanism of ferromagnetism in MnAs is an old matter of debate, which extends to present days. Localized models of MnAs ferromagnetism have been confronted with itinerant models for many years. Although α -MnAs shows metallic conductivity and contains itinerant electrons,⁸ there is increasing evidence^{7,9,10} that ferromagnetic ordering within and in between the hexagonal Mn planes is transmitted by the strongly directional and localized Mn–As–Mn bonds via a double-exchange mechanism,^{11,12} where the parallel spin alignment is promoted by an electron transfer between the localized *d* states of the Mn cations through extended *d* or *p* type states of the anionic As.⁹ The Mn–As–Mn interaction/distance seems to be the key parameter driving the transition from the paramagnetic to the ferromagnetic state. In view of the strong coupling of the structural and magnetic properties of MnAs, incorporation of MnAs in devices, as epitaxially constrained films or as clusters embedded in a matrix, requires a detailed knowledge of the MnAs strain state in these morphologies. The strain state of MnAs clusters embedded in GaAs has long remained unknown, because the relatively weak signal of x-ray diffraction (XRD) in the tiny MnAs crystallites is

shadowed, in conventional x-ray diffraction analysis, by the dominant signals of diffraction in the GaAs matrix and background scattering. In this letter, we report on the room-temperature lattice distortion of MnAs nanocrystals embedded in GaAs, determined through the detection of the x-ray coherent scattering in the nanocrystals.

The sample fabrication process included two steps: Molecular-beam epitaxy growth of a ternary Ga_{1-x}Mn_xAs alloy and subsequent thermal annealing. First, a GaAs buffer layer was grown on a GaAs(001) substrate. The substrate was then cooled down to 300 °C for the growth of ~960 nm of a ternary Ga_{1-x}Mn_xAs alloy with *x* ≈ 0.06. After growth, the sample was annealed *ex situ* in a rapid thermal annealing oven at 700 °C for 20 s. The annealing step gives rise to spherical MnAs crystallites of variable diameter in the range of 20–45 nm embedded in a GaAs matrix, as we observed in transmission electron microscopy analysis.¹³ Superconducting quantum interference device analysis showed the granular GaAs:MnAs film to be ferromagnetic below about 330 K. XRD measurements were carried out in a state-of-the-art PANalytical X'Pert diffractometer system, with a hybrid monochromator, consisting of a multilayer x-ray mirror for parallelization of the divergent beam emitted by the x-ray tube and a grooved Ge crystal acting as a monochromator in combination with that mirror.

The MnAs crystallites are known¹³ to keep a well-defined orientation relationship (nominal orientation) with the GaAs matrix: The (00.1) basal planes of the MnAs crystallites are parallel to {111} GaAs planes, the $\langle 2\bar{1}.0 \rangle$ MnAs basal directions are parallel to $\langle 011 \rangle$ or $\langle 0\bar{1}1 \rangle$ GaAs directions, and the orthogonal $\langle 01.0 \rangle$ MnAs basal directions are parallel to $\langle 1\bar{1}2 \rangle$ GaAs directions.¹⁴ Four possible orientations of the MnAs clusters with respect to the GaAs matrix coexist, corresponding to MnAs (00.1) planes parallel to each of the four GaAs {111} plane orientations. Figure 1 shows a ω - 2θ scan recorded across the GaAs ($2\bar{2}4$) substrate/matrix reflection, in the diffracting plane defined by

^{a)}Electronic mail: mmoreno@icmm.csic.es

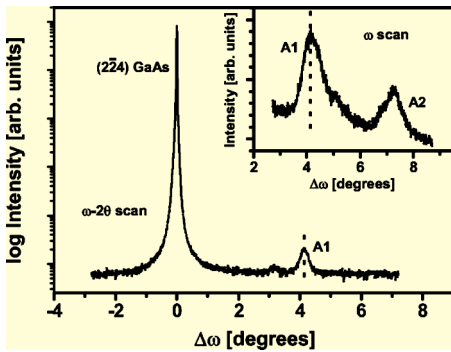


FIG. 1. ω - 2θ scan across the $(2\bar{2}4)$ GaAs reflection and (inset) ω scan across Peak A1.

the $[001]$ and $[\bar{1}10]$ GaAs scattering vectors. A peak (A1) appears aligned with the $(2\bar{2}4)$ GaAs reflection, as confirmed by the ω -scan shown in the inset. A different peak, A2, appears about 3° rotated toward increasing ω angles (inset of Fig. 1). We assign Peak A1 to the (03.0) reflection in MnAs crystallites with basal planes parallel to the $(\bar{1}11)$ GaAs planes. The good alignment—along the ω - 2θ direction—of Peak A1 with respect to the $(2\bar{2}4)$ GaAs reflection indicates that the (01.0) planes of the MnAs crystallites are parallel to the $(\bar{1}\bar{1}2)$ planes of the GaAs matrix, as expected for MnAs crystallites with nominal orientation. Figure 2(a) shows a (01.0) plane within the MnAs unit cell. The (01.0) interplanar distance of the MnAs crystallites is determined to be $d_{(01.0)} = 3.2113 \text{ \AA}$. The distance is smaller than in unstrained bulk MnAs, $d_{(01.0)}^{\text{bulk}} = 3.2205 \text{ \AA}$.¹⁵ The lattice of the MnAs crystallites is compressed by -0.29% in the $[01.0]$ direction.

Figure 3 shows a ω - 2θ scan recorded across the $(0\bar{4}4)$ GaAs reflection, in the diffracting plane defined by the $[001]$ and $[010]$ GaAs scattering vectors. A peak (B) appears aligned with the $(0\bar{4}4)$ GaAs reflection, as confirmed by the ω -scan shown in the inset. We assign Peak B to the $(4\bar{2}.0)$

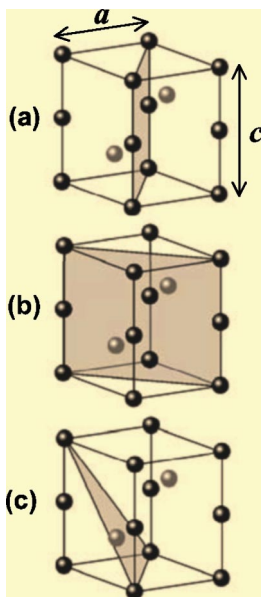


FIG. 2. Hexagonal unit cell of MnAs showing: (a) A (01.0) plane, (b) a $(2\bar{1}.0)$ plane, and (c) a (01.1) plane. Dark (gray) balls represent Mn (As) atoms.

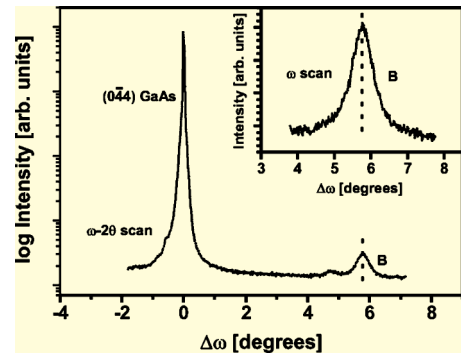


FIG. 3. ω - 2θ scan across the $(0\bar{4}4)$ GaAs reflection and (inset) ω -scan across Peak B.

reflection in MnAs crystallites with basal planes parallel to the $(\bar{1}11)$ GaAs planes. The good alignment—along the ω - 2θ direction—of Peak B with respect to the $(0\bar{4}4)$ GaAs reflection indicates that the $(2\bar{1}.0)$ planes of the MnAs crystallites are parallel to the $(0\bar{1}1)$ GaAs planes. Figure 2(b) shows a $(2\bar{1}.0)$ plane within the MnAs unit cell. The $(2\bar{1}.0)$ interplanar distance of the MnAs crystallites is determined to be $d_{(2\bar{1}.0)} = 1.8538 \text{ \AA}$. The obtained distance is in good agreement with the value we previously found¹⁶ from *grazing incidence* XRD measurements. The interplanar distance in the crystallites is smaller than in unstrained bulk MnAs, $d_{(2\bar{1}.0)}^{\text{bulk}} = 1.8594 \text{ \AA}$.¹⁵ The lattice of the MnAs crystallites is compressed by -0.30% in the $[2\bar{1}.0]$ direction. The approximately equal values of the strain along the $[01.0]$ and $[2\bar{1}.0]$ directions indicate that the MnAs crystallite structure keeps a hexagonal symmetry; no orthorhombic deformation occurs.

In order to complete the analysis of the crystallite structure in three orthogonal directions, determination of the interplanar spacing along the c axis remains. We searched for the (01.1) reflection near the (002) GaAs reflection. We recorded ω and ω - 2θ scans in this region, shown in Fig. 4, using the (002) GaAs reflection as reference. The ω -scan of Fig. 4 shows two peaks, C1 and C2, that appear rotated toward positive ω values relative to the (002) GaAs reflection. We assign Peak C1 to the (01.1) reflection in MnAs clusters whose basal planes are parallel to the $(1\bar{1}1)$ GaAs planes. A MnAs (01.1) plane is shown in Fig. 2(c). The (01.1) interplanar distance corresponding to nominally oriented crystallites is determined to be $d_{(01.1)} = 2.8112 \text{ \AA}$. The (00.1) inter-

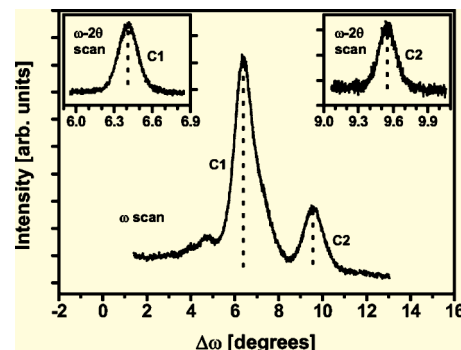


FIG. 4. ω scan across Peaks C1 and C2 and (insets) ω - 2θ scans across Peaks C1 and C2, respectively.

TABLE I. Nearest-neighbors distances and unit-cell volume in MnAs.

	MnAs clusters ($\sim 20^\circ\text{C}$)	Bulk α -MnAs ($\sim 20^\circ\text{C}$)	Bulk α -MnAs ($\sim 39^\circ\text{C}$)	Bulk α -MnAs ($\sim 39^\circ\text{C}$)
Mn–Mn (<i>c</i> axis) (\AA)	2.908	2.851 ^c	2.860 ^a	2.860 ^a
Mn–Mn (<i>a</i> axis) (\AA)	3.708	3.719 ^c	3.715 ^a	3.681 ^a
Mn–As (\AA)	2.588	2.577 ^c	2.58 ^b	2.52–2.61 ^b
Volume (\AA^3)	34.62	34.15 ^c	34.19 ^a	33.57 ^a

^aSee Ref. 4.^bSee Ref. 6.^cSee Ref. 17.

planar spacing is then calculated from the already known (01.0) and (01.1) spacings. The obtained value, $d_{(00.1)} = 5.8156 \text{ \AA}$, is considerably larger than the spacing corresponding to bulk MnAs, $d_{(00.1)}^{\text{bulk}} = 5.7024 \text{ \AA}$.¹⁵ The lattice of the MnAs crystallites is expanded by as much as 1.99% along the *c* axis. We assign Peaks A2 and C2 to the (01.5) and (01.1) reflections, respectively, in MnAs clusters whose (00.1) basal planes are not exactly parallel to the (1 $\bar{1}$ 1) GaAs planes, but about 3° rotated toward (001) GaAs. Very small peaks appearing in Figs. 1, 3, and 4—other than those already mentioned—are too weak for a definite assignment. These peaks could correspond to other cluster orientations, or to other cluster phases, or they could be diffuse scattering features. They represent a minor contribution.

Table I lists the room-temperature nearest-neighbors distances as well as the unit-cell volume derived from the x-ray results for the nominally oriented crystallites, as well as the values reported in the literature for bulk α -MnAs at room temperature, and for the α and β phases of bulk MnAs at the phase-transition temperature. Along the *c* axis, the Mn–Mn distance is substantially larger in the crystallites than in bulk MnAs. In the basal planes, the Mn–Mn distance is slightly shorter in the crystallites than in bulk α -MnAs. The Mn–As distance is substantially larger in the crystallites than in bulk α -MnAs; the large lattice expansion along the *c* axis overcompensates for the shortening of the Mn–As distance due to the compression in the basal planes. The strains of the crystallites at room temperature result from the combination of the “initial” strains generated in the precipitation process, and the strains generated during sample cooling because of: (i) The different thermal expansion of MnAs and GaAs and (ii) the MnAs abrupt volume change across the first-order phase transition. The magnetic properties of MnAs are known to be enhanced for larger unit-cell volume and reduced *p*-*d* hybridization.^{5,7,18,19} The increased first nearest-neighbors Mn–Mn and Mn–As distances in the crystallites are expected to result in reduced *d*-*d* overlap and reduced *p*-*d* hybridization, thus giving rise to improved magnetic properties as compared to unstrained bulk α -MnAs. Leaving aside effects related to the small crystallite size, ferromagnetism in the strained crystallites is expected to be more stable than in bulk α -MnAs. This is supported by the phase-transition temperature measured for GaAs:MnAs $T_C \approx 330 \text{ K}$,²⁰ which is about 17°C higher than in bulk MnAs.

In summary, we have detected the x-ray coherent scattering in MnAs nanosized crystallites embedded in a GaAs

matrix, and we have determined the room-temperature interatomic distances along three orthogonal directions of the crystallites. The MnAs grains are found to be under a high anisotropic strain; the hexagonal symmetry being maintained. The appearance of ferromagnetic order, with enhanced stability, in the strained MnAs crystallites supports the localized double-exchange models of MnAs ferromagnetism.

This work has been partly supported by the CSIC/European Social Fund through the I3P Program, by the European Commission through the Human Resources and Mobility activity under Contract No. MERG-CT-2004-6373, and by the Spanish Ministerio de Educación y Ciencia under Grant No. MAT 2004–5348.

¹J. De Boeck, R. Oesterholt, A. Van Esch, H. Bender, C. Bruynseraede, C. Van Hoof, and G. Borghs, *Appl. Phys. Lett.* **68**, 2744 (1996).²H. Shimizu, M. Miyamura, and M. Tanaka, *Appl. Phys. Lett.* **78**, 1523 (2001).³C. Pampuch, A. K. Das, A. Ney, L. Däweritz, R. Koch, and K. H. Ploog, *Phys. Rev. Lett.* **91**, 147203 (2003).⁴B. T. M. Willis and H. P. Rooksby, *Proc. Phys. Soc. London, Sect. B* **67**, 290 (1954).⁵C. P. Bean and D. S. Rodbell, *Phys. Rev.* **126**, 104 (1962).⁶R. H. Wilson and J. S. Kasper, *Acta Crystallogr.* **17**, 95 (1964).⁷N. Menyuk, J. A. Kafalas, K. Dwight, and J. B. Goodenough, *Phys. Rev.* **177**, 942 (1969).⁸S. Haneda, N. Kazama, Y. Yamaguchi, and H. Watanabe, *J. Phys. Soc. Jpn.* **42**, 1201 (1977).⁹K. Bärner, *Phys. Status Solidi B* **88**, 13 (1978).¹⁰A. K. Das, C. Pampuch, A. Ney, T. Hesjedal, L. Däweritz, R. Koch, and K. H. Ploog, *Phys. Rev. Lett.* **91**, 087203 (2003).¹¹C. Zener, *Phys. Rev.* **82**, 403 (1951).¹²P. W. Anderson and H. Hasegawa, *Phys. Rev.* **100**, 675 (1955).¹³M. Moreno, A. Trampert, B. Jenichen, L. Däweritz, and K. H. Ploog, *J. Appl. Phys.* **92**, 4672 (2002).¹⁴We use the (*hkl*) “four-indices notation” for the MnAs planes, omitting the third index $i = -(h+k)$.¹⁵The unstrained lattice parameter in a certain direction, d_0 , is calculated using the bulk a_0 and c_0 lattice parameters reported by J. Mira, F. Rivadulla, J. Rivas, A. Fondado, T. Guidi, R. Caciuffo, F. Carsughi, P. G. Radaelli, and J. B. Goodenough, *Phys. Rev. Lett.* **90**, 097203 (2003).¹⁶M. Moreno, B. Jenichen, V. Kaganer, W. Braun, A. Trampert, L. Däweritz, and K. H. Ploog, *Phys. Rev. B* **67**, 235206 (2003).¹⁷J. Mira, F. Rivadulla, J. Rivas, A. Fondado, T. Guidi, R. Caciuffo, F. Carsughi, P. G. Radaelli, and J. B. Goodenough, *Phys. Rev. Lett.* **90**, 097203 (2003).¹⁸S. Sanvito and N. A. Hill, *Phys. Rev. B* **62**, 15553 (2000).¹⁹A. Continenza, S. Picozzi, W. T. Geng, and A. J. Freeman, *Phys. Rev. B* **64**, 085204 (2001).²⁰M. Moreno, A. Trampert, L. Däweritz, and K. H. Ploog, *Appl. Surf. Sci.* **234**, 16 (2004).